

# Outstanding HC-SCR of Lean NO<sub>x</sub> Over Pt/Mesoporous-Silica Catalysts

Tamikuni Komatsu\*, Keizou Tomokuni, Mitsuo Konishi and Takashi Shirai

The Noguchi Institute, Asahi-Kasei Corporation, 1-8-1 Kaga, Itabashi-Ku, Tokyo 173-0003, Japan

**Abstract:** Perfect de-NO<sub>x</sub> over a wide temperature range above 170 °C was achieved using a new Pt-catalyst supported on mesoporous silica (Pt/MPS) and a stoichiometric amounts of long-chain hydrocarbons as reducing agents for NO<sub>x</sub>-purification. Kinetic investigation of the HC-SCR of lean NO<sub>x</sub> over Pt/MPS, Pt/alumina and Pt/zirconia showed that such a remarkable activity of Pt/MPS is due to a large frequency factor but not to activation energy. Acid-treatment of the supports increased the activities of the catalysts and generated new IR-peaks in the range 1000-1200 cm<sup>-1</sup>, which suggests the support-effects on the catalyst-activities to be related to the special surface functional groups of the supports. The present HC-SCR must be very useful to remove diesel-NO<sub>x</sub> by means of pulse-injection of diesel fuel into the exhaust.

**Keywords:** HC-SCR, lean NO<sub>x</sub>, de-NO<sub>x</sub>, diesel exhaust, mesoporous, mesoporous silica, diesel fuel.

## INTRODUCTION

The regulation of greenhouse warming due to CO<sub>2</sub> discharged by automobiles has become quite severe all over the world. To decrease CO<sub>2</sub> emission, changes such as gasoline-autos into diesel-autos with higher fuel efficiency have been expected. However, how to purify diesel-NO<sub>x</sub> is still unresolved. The O<sub>2</sub>-content of the gasoline-exhaust is controlled below 0.5% (rich burn) but the O<sub>2</sub>-content of the diesel-exhaust is usually 24% O<sub>2</sub> (lean burn). This makes purification of the diesel-NO<sub>x</sub> very difficult, because of immediate deactivation of the conventional three-way catalysts by oxygen at 1%. Also, comparatively low temperatures of the diesel-exhaust which are usually 100-400 °C make purification very difficult because of the low activities of the conventional catalysts below 200 °C. Diesel-fuel consists of C<sub>6</sub>-C<sub>16</sub> HCs including aromatic compounds. However, the fuel was not directly used as the reducing agents because of low reducing performance, while a usage of diesel-fuel for reduction of NO<sub>x</sub> is essentially necessary for such de-NO<sub>x</sub> catalysts as remove NO<sub>x</sub> by means of pulse-injection of diesel-fuel into the exhaust.

The recent de-NO<sub>x</sub> methods such as the urea-SCR and NO<sub>x</sub>-storage-reduction (LNT: lean-NO<sub>x</sub>-trap) were reviewed [1]: (1) the urea-SCR has unresolved problems that the method requires storing a solution of urea and that a large portion of NO<sub>x</sub> may be discharged in the form of nitrates and nitrites at low temperatures; (2) the LNT has essential problems such as deactivation of NO<sub>x</sub>-storage agents by a small SO<sub>x</sub>-content and very low activities below 200 °C. The other method, the HC-SCR [2-6] has a problem that the purification is limited to narrow temperature ranges around 200 °C, although the catalysts are free from deactivation by SO<sub>x</sub> [7]. To improve the HC-SCR method, the presentation of Pt-catalysts supported on MCM-41 type mesoporous silica [8], the intermediate addition of reducing agents [9], a secondary fuel-injection method [10], a double-

washed honeycomb coating with two kinds of Pt-catalysts [11], and a fast SCR process [12] were studied. However, the HC-SCR method has not been considered for mainstream lean burn NO<sub>x</sub>-purification, because of the low activities of the catalysts below 200 °C and a narrow temperature window.

Previously, we presented outstanding low-temperature active Pt/MPS to purify diesel-NO<sub>x</sub> exhaust [13]. The present study will report the kinetics of HC-SCR of NO<sub>x</sub> over Pt/MPS and an application to perfect purification of diesel-NO<sub>x</sub> in a wide temperature range over 170 °C with diesel-fuel.

## MATERIALS AND METHODOLOGY

### Sample Preparation

Mesoporous silica (MPS) was prepared by a sol-gel method using tetraethyl orthosilicate (TEOS) as a silica-source and dodecylamine as a template. Pt/MPS was prepared by impregnating MPS with an aqueous solution of H<sub>2</sub>PtCl<sub>4</sub> as the Pt-source. The experimental details were described in the previous report [13]. For comparison, Pt/silica, Pt/silica-alumina, Pt/alumina, Pt/zirconia and a NO<sub>x</sub>-absorption-reduction catalyst (LNT) were prepared in a similar manner as above using commercially available support-materials. The precious metal loading was 5 mass % Pt and 0.3 mass % Rh for Pt/MPS, and 2 mass % Pt and 0.12 mass % Rh for Pt/silica, Pt/silica-alumina, Pt/alumina and Pt/zirconia. The LNT was 2%Pt-0.12%Rh/alumina (80%)-ceria (10%)-zirconia (10%) including BaCO<sub>3</sub> (3%), La<sub>2</sub>O<sub>3</sub> (1%) and KOH (1%). In addition, Pt-catalysts using acid-treated supports of MPS, γ-alumina and zirconia were also prepared. The acid-treatment of the supports was carried out as follows: boiling in a 0.1 mass % solution of equimolar HNO<sub>3</sub> and H<sub>2</sub>SO<sub>4</sub> for 3 h, followed by washing with distilled water. A honeycomb catalyst was prepared using the Pt/MPS powders as follows: a slurry of the Pt/MPS powders mixed with alumina-sol was prepared, coated on a full-size cordierite-honeycomb (φ143.8 mm×118 mm, 4.5 mil/400 cpsi), followed by calcination at 600 °C for 1h in air. A coating mass of Pt/MPS was 80 g per 1 liter of the

\*Address correspondence to this author at 2-24-4 Sakura, Tsukuba-shi, Ibaraki 305-0003, Japan; Tel: +81 29-857-7325; Fax: +81 29-857-7325; E-mail: BRA01367@nifty.com

honeycomb. Assessment of the heat-resistance of Pt/MPS was carried out using the sample after the heat-treatment under each condition of 600 °C-50 h, 700 °C-50 h and 800 °C-50 h in air containing 10% steam.

### Characterization of the Samples

The specific surface areas and pore sizes of the supports were measured using nitrogen adsorption at 77 K. The pore-structure of the supports was characterized by small-angle X-ray diffraction (SAX) and selected-area electron diffraction (SAED). Exposed active sites of Pt/MPS for estimation of turn over frequency (ToF) were measured by CO-chemisorption. Crystallite sizes of the catalysts were directly measured by high-resolution TEM (HRTEM) observation. The average size of the crystallites was estimated from the half-width of the (111) reflection by powder XRD measurements. Homogeneities of the supported catalysts were confirmed by HRTEM observations.

### Measurements of HC-SCR of NO<sub>x</sub>

The experiment of HC-SCR of NO<sub>x</sub> was carried out using a three-necked quartz tubular downflow reactor (20 mm i.d and 400 mm length). A mini honeycomb-catalyst (2 ml in volume) or powder catalyst was charged into the reactor, a small amount of glass wool was placed on the catalyst, and 10 ml of sea-sand<sup>1</sup> as a dispersant of reaction gases was placed on the glass wool to initiate the reaction over the catalyst in a homogeneous reaction gas flow. The mini honeycomb catalyst was cut from the full-size honeycomb catalyst. The powder catalyst (160 mg of 5% Pt-catalysts or 400 mg of 2% Pt-catalysts) was mixed in advance with commercially available sea-sand (20-30 mesh) at 2.6 g (2 ml) and charged into the reactor. The reactor containing the catalyst was placed in an electric furnace. As an exhaust gas for NO<sub>x</sub>-purification experiments, three model-gases, (1) a reaction mixture comprising 250 ppm NO, 400 ppm C<sub>3</sub>H<sub>6</sub> and 10% O<sub>2</sub> balanced with He, (2) a reaction mixture comprising 250 ppm NO<sub>2</sub>, 400 ppm C<sub>3</sub>H<sub>6</sub> and 10% O<sub>2</sub> balanced with He, (3) a reaction mixture comprising 250 ppm NO, 2000-7000 ppm liquid of long chain HCs and 10% O<sub>2</sub> balanced with He, were used. Each model-gas was introduced into a gas-inlet of the reactor at a flow rate of 1000 ml min<sup>-1</sup> (SV=30,000 h<sup>-1</sup> or GHSV=7.5 m<sup>3</sup> h<sup>-1</sup> per g of Pt) through a mass-flow controller. The liquid HCs were supplied upstream along the inner wall of the reactor by a syringe-type micro-feeder. The temperature of the reactor was increased at a rate of about 10 °C min<sup>-1</sup> and was held at the prescribed temperature for 10 min. The NO<sub>x</sub> measurement of the effluent gas was carried out during a period held at the prescribed temperature using a chemiluminescence NO<sub>x</sub>-detector<sup>2</sup>. To confirm the mechanism of the HC-SCR, two reactors containing the honeycomb catalyst were connected in series. The first stage (oxidation of NO into NO<sub>2</sub> with O<sub>2</sub>) was carried out by introducing a reaction mixture of 250 ppm NO and 10% O<sub>2</sub> balanced with He into the gas-inlet of the first-stage reactor at a flow rate of 1000 ml min<sup>-1</sup> (SV=30,000 h<sup>-1</sup>) and the

second stage (reduction of NO<sub>x</sub> with propylene) was carried out by introducing 400 ppm C<sub>3</sub>H<sub>6</sub> into the gas-inlet of the second-stage reactor at a flow rate of 1000 ml min<sup>-1</sup>. The result was analyzed using the experimental NO<sub>x</sub>-conversion and NO:NO<sub>2</sub> ratio<sup>3</sup>.

## RESULTS AND DISCUSSION

### Characterization of the Pt-Catalysts

Table 1 shows the characterization of the used Pt-catalysts and supports. The SAX profile of MPS showed a strong singlet-peak at 2θ=2.72 °(d=3.25 nm). The SAED image showed a hallow pattern. The results mean that MPS is completely disordered in the pore-arrangement differently from well-ordered MCM-41. The specific surface area and pore diameter of MPS were 1250 m<sup>2</sup> g<sup>-1</sup> and 2.5 nm, respectively. An estimated thickness of mesopore-walls for MPS was ca. 2 nm, which is about twice larger than that for MCM-41. Relative IR-intensity around at 3400 cm<sup>-1</sup> showed that MPS is covered with minor amount of hydrolytic OH-groups in comparison to MCM-41. The exposed active site of Pt/MPS which was estimated from the experimental CO-chemisorption was ca. 5%. The HRTEM image of Pt/MPS indicated that many Pt-particles of 1-3 nm in diameter are homogeneously dispersing on the support surface. The average diameter of the Pt-particles was 2 nm which is very close to the pore diameter of MPS. This indicates the Pt-particles of the catalyst to be supported in the inside of mesopores. On the other hand, those for Pt/alumina, Pt/silica-alumina, Pt/silica, LNT and Pt/zirconia were 2, 4, 5, 6 and 21 nm, respectively. Since the average diameter of Pt/silica-alumina is smaller than the pore diameter, the Pt-particles of the catalyst may be in the inside of mesopores. However for Pt/silica and Pt/zirconia, the Pt-particles are supported in the outside of mesopores. Also, the Pt-particles of Pt/alumina and LNT may be supported in the outside of mesopores, because adsorption ability of γ-alumina is much stronger than those of the other supports.

**Table 1. Characterization of the Used Pt-Catalysts (Powders) and Supports**

Pt-Catalysts	Pt-Particles Average Diameter/nm	Support	
		Specific Surface Area/m <sup>2</sup> g <sup>-1</sup>	Pore Diameter/nm
Pt/MPS	2	1250	2.5
Pt/Silica	5	428	non-porous
Pt/Silica-Alumina	4	412	3.8
Pt/Alumina	2	250	6.2
Pt/Zirconia	21	128	7
LNT Type Catalyst	6	210	6-20

### Heat-Resistance of MPS and Pt/MPS

The specific surface areas and poresizes of MPS before and after the heat-treatment at 700 °C-50 h in air containing

<sup>1</sup>Sea-sand (quartz-sand) is generally used as a dispersant because of inactivity in catalysis.

<sup>2</sup>The diminished-pressure chemiluminescence NO<sub>x</sub> detector, Japan Thermo Corp. Model 42 i—HL & 46 C—H, which performs simultaneous detection of NO, NO<sub>2</sub> and N<sub>2</sub>O contained in the effluent gas.

<sup>3</sup> From the experimental NO<sub>x</sub>-conversion and NO : NO<sub>2</sub> ratio, contribution of NO or NO<sub>2</sub> to the NO<sub>x</sub>-conversion can be estimated, since NO<sub>x</sub>-conversion is defined as the conversion of NO<sub>x</sub> (total of NO and NO<sub>2</sub>) into nonhazardous N-containing compounds such as N<sub>2</sub> and N<sub>2</sub>O.

10% steam were almost unchanged. The hydrothermal durability of MPS was much higher than that of MCM-41. According to our experiment, MCM-41 lost half of the specific surface area and mesopores after ageing at 600 °C-24 h in air containing 10% steam. Probably the high heat-resistance of MPS is due to the thick mesopore-walls and minor amounts of hydrolytic OH-groups, because under hydrothermal conditions H<sub>2</sub>O molecules attacks -Si-O-skeletons to destroy mesoporous structures. Fig. (1) shows the relationship between NO<sub>x</sub>-conversion and ageing conditions for Pt/MPS. Until 600 °C-50 h, a maximum NO<sub>x</sub> conversion (70%) and corresponding temperature (the lower limit in temperature: 170 °C) were similar to those of fresh Pt/MPS. After 700 °C-50 h, the NO<sub>x</sub> conversion was not changed but the lower limit in temperature rose to 210 °C (40 °C rise). After 800 °C-50 h, the NO<sub>x</sub> conversion dropped to 45% (25% drop) and the lower limit in temperature rose to 230 °C (60 °C rise). In order to elucidate whether such a higher temperature shift is due to permanent deterioration or not, the heat-treated Pt/MPS was reduced with hydrogen at 300 °C-1 h, followed by the same HC-SCR of NO<sub>x</sub>. The result showed remarkable restoration close to the temperature for fresh Pt/MPS. On the other hand, the powder XRD measurements of the heat-treated Pt/MPS showed that an averaged size of Pt-particles was scarcely changed until 600 °C-50 h, increased to 4-5 nm (3 times larger than that of fresh Pt/MPS) after 700 °C-50 h, remarkably increased to 10 nm after 800 °C-50 h. The result teaches that the higher temperature shift for the heat-treated Pt/MPS is due to both oxidation and enlargement of the supported Pt-particles. The former factor may be gradually restored by reduction with HCs contained in rich burn exhausts and the latter greatly influences the activity of the catalyst over 800 °C. A similar relationship between the Pt-size and ageing conditions was observed for conventional Pt/alumina. The high heat resistance of Pt/MPS is found due to mechanically strong encapsulation in the mesopores which is different from chemically strong adsorptive ability of  $\gamma$ -alumina supports, because MPS is much inferior to  $\gamma$ -alumina with respect to adsorptive ability. The activity of Pt/MPS remaining after ageing at 700 °C-50 h corresponds to an estimation of a million km-traveling on the heavy duty diesel cars, on the basis of the Arrhenius plots (the logarithm of ageing hour vs 1/T relationships in the range 400 - 700 °C).

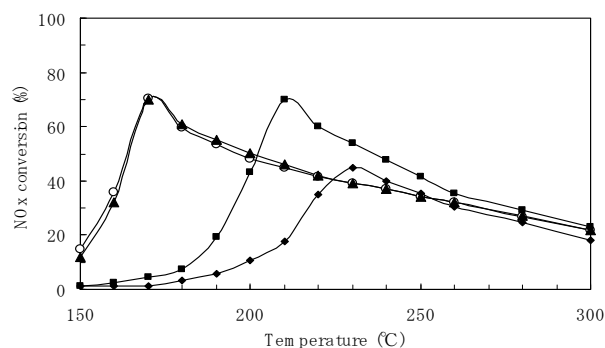


**Fig. (1).** The heat-resistance of Pt/MPS (powders): (○) fresh; (▲) after 600 °C-50 h in air containing 10% steam; (■) after 700 °C-50 h in air containing 10% steam; (◆) after 800 °C-50 h in air containing 10% steam.

### Kinetics of HC-SCR of Lean-NO<sub>x</sub> over the Pt-Catalysts with Propylene

Fig. (2) shows the NO<sub>x</sub>-conversion over Pt/MPS, Pt/alumina and Pt/zirconia using model-gas (1). Pt/MPS provides a peak NO<sub>x</sub>-conversion of 70% at 170 °C, while Pt/alumina and Pt/zirconia respectively show 40% at 240 °C and 33% at 260 °C. The ToF of Pt/MPS in terms of NO<sub>x</sub> conversion, which was calculated on the basis of the experimental exposed active sites, was 0.7 at 70%

NO<sub>x</sub>-conversion. The gas after the treatment was composed of N<sub>2</sub>, N<sub>2</sub>O, CO<sub>2</sub> and H<sub>2</sub>O, except for unchanged NO<sub>x</sub>. The selectivity for N<sub>2</sub> was 10-30% below 200 °C and over 95% above 250 °C, which was almost the same as the selectivity of the gasoline-auto emission purification over the conventional three-way-catalysts. The curve of NO<sub>x</sub>-conversion before the peak for each catalyst is almost the same as that of NO-conversion, that is, the NO<sub>x</sub>-conversion is almost the same as the conversion of NO<sub>2</sub>. After the peak, the NO-conversion continues to increase up to 250 °C followed by a slight decrease above 250 °C. The NO<sub>x</sub>-conversion tends to decrease after the peak, which means that an increase in NO<sub>2</sub> does not contribute to the NO<sub>x</sub>-conversion. This is due to wasteful consumption of propylene above 180 °C, because propylene is very combustible with oxygen. According to our experiment, the conversion of propylene over Pt/MPS with 10% O<sub>2</sub> begins at 100 °C and increases rapidly at 110 °C, reaching 100% at 150 °C. Apparent activation energies and frequency factors estimated from the conversion curve were 104 kJ mol<sup>-1</sup> and 2.4×10<sup>7</sup> s<sup>-1</sup>, respectively. The smaller NO<sub>x</sub>-conversions of Pt/alumina and Pt/zirconia are not only due to the low activities of the catalysts but also to unselective conversion of propylene above 200 °C.

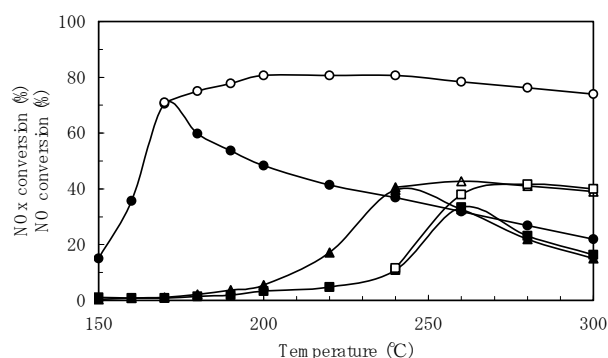


**Fig. (2).** NO<sub>x</sub>-conversion over the Pt-catalysts (powders) with model-gas (1): (●), (▲) and (■) depict the NO<sub>x</sub>-conversion over Pt/MPS, Pt/alumina and Pt/zirconia, respectively; (○), (△) and (□) depict the NO-conversion over the Pt/MPS, Pt/alumina and Pt/zirconia, respectively.

Fig. (3) shows the Arrhenius plots (the logarithm of conversion rate vs 1/T relationships) of the observed NO<sub>x</sub>-conversions shown in Fig. (2). The obtained apparent activation energies *E* and frequency factors *A* are summarized in Table 2. These results show that the *E*-values for NO<sub>x</sub>-conversions of Pt/MPS, Pt/alumina and Pt/zirconia are scarcely different. The obtained values are slightly different from those reported previously [14-17] (*E*<sub>NO</sub>=91.2

$\text{kJ mol}^{-1}$  and  $E_{\text{C}_3\text{H}_6}=108.5 \text{ kJ mol}^{-1}$  reported by Ioan *et al* [14]), because of the different reaction conditions. The A-value of Pt/MPS is larger by at least two orders of magnitude than those of Pt/alumina and Pt/zirconia. Therefore, the difference in activity among the catalysts must be affected by frequency factors rather than activation energies. On the other hand, the Pt-particle size of Pt/MPS is similar to that of Pt/alumina as shown in Table 1. The results suggest that the remarkable low-temperature activity of Pt/MPS is due to the MPS-support.

**Table 2. Apparent Activation Energies and Frequency Factors of Pt-Catalysts (Powders) Estimated from Fig. (2)**

Pt-Catalysts	NO <sub>x</sub> -Conversion		C <sub>3</sub> H <sub>6</sub> -Conversion	
	E/kJ mol <sup>-1</sup>	A/s <sup>-1</sup>	E/kJ mol <sup>-1</sup>	A/s <sup>-1</sup>
Pt/MPS	102	$8.6 \times 10^6$	124	$1.4 \times 10^9$
Pt/Alumina	102	$2.6 \times 10^4$	—	—
Pt/Zirconia	101	$5.9 \times 10^3$	—	—

Estimations of E and A of the C<sub>3</sub>H<sub>6</sub> conversion for Pt/alumina and Pt/zirconia were useless because of wasteful combustion of propylene above 200 °C.

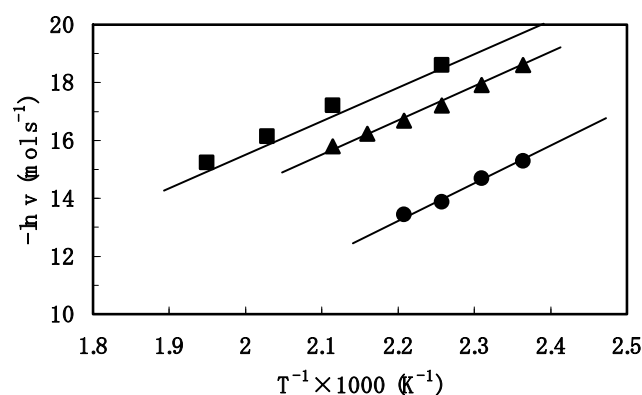


**Fig. (3).** Arrhenius plots (the logarithm of conversion rate vs 1/T relationships) of the observed NO<sub>x</sub>-conversions over Pt/MPS, Pt/alumina and Pt/zirconia shown in Fig. (2): (●) Pt/MPS; (▲) Pt/alumina; (■) Pt/zirconia.

### The Effects of Supports on NO<sub>x</sub>-Conversion

To clarify the above effects of supports to the NO<sub>x</sub>-conversion, acid-treatment of the supports was carried out. Fig. (4) shows the NO<sub>x</sub>-conversions over the Pt-catalysts using acid-treated  $\gamma$ -alumina and zirconia. As seen from the comparison with Fig. (2), the acid-treatment of the supports gives a remarkable increase in NO<sub>x</sub>-conversion and low-temperature shifts of the peak-temperatures. The acid-treatment of MPS also increases the NO<sub>x</sub>-conversion by several %. The IR spectra of  $\gamma$ -alumina and zirconia after the acid-treatment were investigated. Resultantly, new peaks appeared at 1152 and 1065  $\text{cm}^{-1}$  for  $\gamma$ -alumina and 1211, 1141 and 1047  $\text{cm}^{-1}$  for zirconia. Since the absorption bands in this finger-print region are generally assigned to the stretching bands of SiO<sub>2</sub>-skelton, the observed peaks are probably due to protons bonded to the metal oxide skeletons because stretching bands of Si-O in Si-OH groups are generally known to be observed in the range 800-1000  $\text{cm}^{-1}$ .

It is also well-known that a portion of active OH-groups on solid-acids is acting as the Brønsted-acid sites. Then, the high activity of Pt/MPS and increased activities of Pt/alumina and Pt/zirconia using the acid-treated supports are probably due to active protons incorporated with the supports.

### Mechanism of the HC-SCR of Lean-NO<sub>x</sub>

To elucidate a mechanism of the HC-SCR of NO<sub>x</sub> over Pt/MPS, the NO<sub>x</sub>-purification process was formally divided into two stages: (1) [1<sup>st</sup>-stage] oxidation of NO into NO<sub>2</sub>

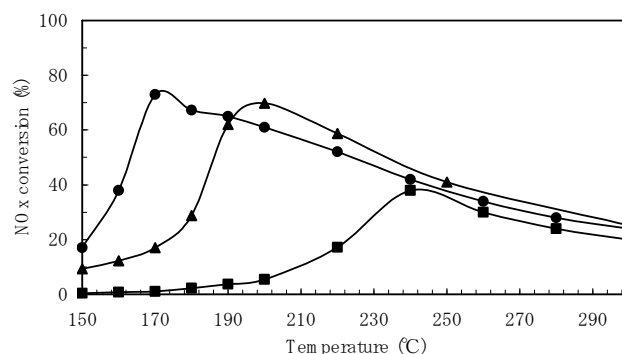


**Fig. (4).** NO<sub>x</sub>-conversion over the Pt-catalysts (powders) supported on acid-treated supports with model-gas (1): (●), (▲) and (■) depict the NO<sub>x</sub>-conversion over Pt/[acid-treated MPS], Pt/[acid-treated alumina] and Pt/[acid-treated zirconia], respectively.

with O<sub>2</sub>, (2) [2<sup>nd</sup>-stage] successive reduction of NO<sub>x</sub> with propylene. From Fig. (5a), it is found that Pt/MPS slowly oxidizes NO to NO<sub>2</sub> with O<sub>2</sub>, because the conversion of NO to NO<sub>2</sub> is much lower than that predicted from the equilibrium. The apparent activation energies and frequency factors estimated from Fig. (5a) were 108  $\text{kJ mol}^{-1}$  and  $5 \times 10^4 \text{ s}^{-1}$ , respectively. Fig. (5b) shows that all of the NO<sub>2</sub> produced in the first stage is reduced into N<sub>2</sub>O and N<sub>2</sub> below 170 °C, because the NO<sub>2</sub> ratio is zero % from the beginning of reaction (150 °C) to a maximum NO<sub>x</sub> conversion (170 °C). Fig. (5c) shows the result of HC-SCR of NO<sub>2</sub> over Pt/MPS with propylene. The estimated apparent activation energy was 64  $\text{kJ mol}^{-1}$ . That is, [2<sup>nd</sup>-stage] reduction of NO<sub>2</sub> with propylene is very faster than [1<sup>st</sup>-stage] oxidation of NO into NO<sub>2</sub>. Therefore, oxidation of NO into NO<sub>2</sub> is the rate-determining step. The results also notify that NO<sub>2</sub>-molecules can be purified into N<sub>2</sub>O and N<sub>2</sub> over Pt-catalysts with HCs but NO-molecules are difficult. The appearance of the Brønsted-acid sites on the acid-treated supports may influence the rate-determining step. If NO<sub>2</sub> is more effective for NO<sub>x</sub>-conversion than NO, the HC-SCR of NO<sub>2</sub> may be more advantageous than that of NO, as reported in ref. [5]. As shown in Fig. (5c), in spite of the HC-SCR of NO<sub>2</sub> ( $E_{\text{NO}_x} = 64 \text{ kJ mol}^{-1}$ ) much faster than that of NO, the maximum NO<sub>x</sub>-conversion (75%) and its temperature (170 °C) were not much different from those for the HC-SCR of NO. Reduction of NO<sub>2</sub> into NO quickly occurred around 150-160 °C (the conversion of NO<sub>2</sub> into NO was 77% at 150 °C). That is, the HC-SCR of NO<sub>2</sub> over Pt/MPS is also unselective. The following is a reaction diagram of the HC-SCR of lean-NO<sub>x</sub> over Pt/MPS which was confirmed from the results.

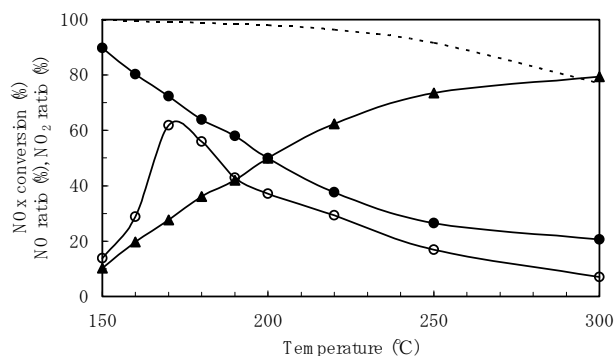
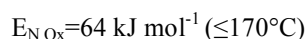
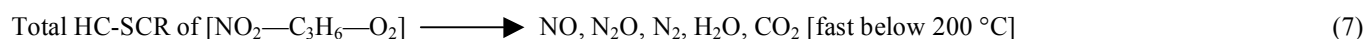
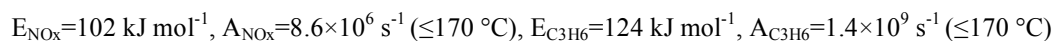
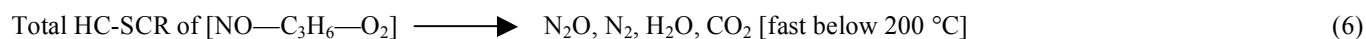
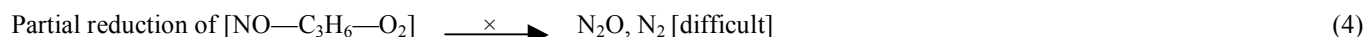
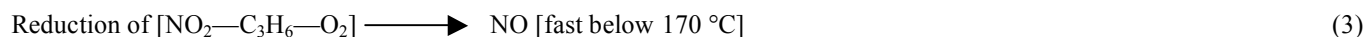
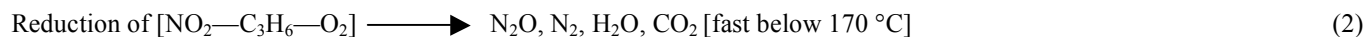
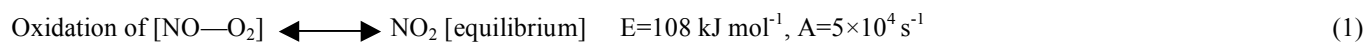


**Fig. (5a).** [1<sup>st</sup> stage] oxidation of NO into NO<sub>2</sub> over Pt/MPS (honeycomb) with O<sub>2</sub>: (●) and (▲) depict the NO ratio and NO<sub>2</sub> ratio, respectively; (---) the equilibrium between NO<sub>2</sub> and NO (ref. [5]). The result of the second stage is also shown: (○) NOx-conversion by injection of C<sub>3</sub>H<sub>6</sub> into the first stage outlet-gas.

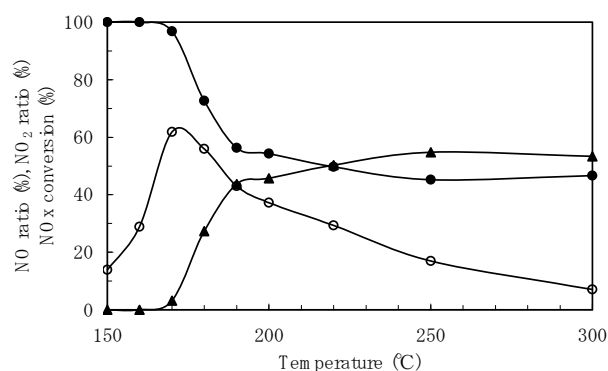
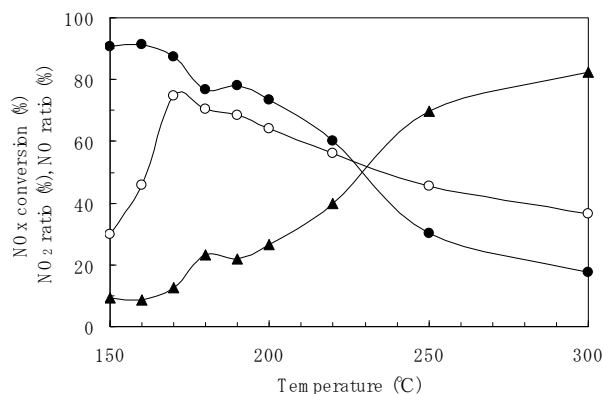


**Fig. (5b).** [2<sup>nd</sup> stage] reduction of the 1<sup>st</sup> stage outlet-gas over Pt/MPS (honeycomb) with propylene: (●) and (▲) depict the NO ratio and NO<sub>2</sub> ratio, respectively; (○) NOx-conversion.

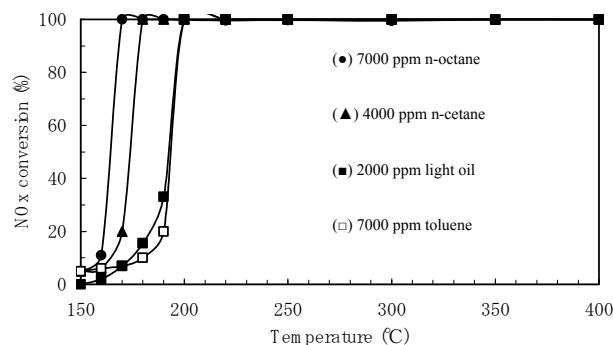
### HC-SCR of Lean-NOx over Pt/MPS with Long-Chain HCs

Fig. (6) shows the purification of NOx over Pt/MPS using model-gas (2). The results show that Pt/MPS is able to perfectly purify lean NOx with stoichiometric HCs (where, stoichiometric HCs mean the quantitative HCs required for the perfect consumption of HC with 10% O<sub>2</sub>) above 170 °C. The apparent order of the reducing activities among the hydrocarbons (in regard to the temperature acting as a reducing agent of NOx) was propylene (100% in NOx-conversion at 170 °C) and n-octane (100% at 170 °C)

> n-cetane (100% at 180 °C) > light oil (100% at 200 °C) and toluene (100% at 200 °C). The NOx-conversion curves and the hydrocarbon-consumption curves were synchronized with each other. The steep slope  $[\Delta(\text{NOx-conversion})/\Delta T]$  of each NOx-conversion curve is almost the same 10% K<sup>-1</sup> for each HC. The results show that the HC-SCR of lean NOx with stoichiometric HCs proceeds rapidly with the catalytic consumption of HCs. Many HCs are combustible over Pt/MPS with excess amounts of oxygen at comparatively mild temperatures. The difference in reducing activity among HCs is not clearly associated with the chain-length of HCs. Most aliphatic and aromatic HCs can be used as the reducing agents for lean NOx over Pt/MPS.



**Fig. (5c).** HC-SCR of NO<sub>2</sub> over Pt/MPS (honeycomb) with model-gas (2): (●) and (▲) depict the NO-ratio and NO<sub>2</sub>- ratio, respectively; (○) NOx-conversion.



**Fig. (6).** HC-SCR of lean NOx over Pt/MPS (honeycomb) with model-gas (3) containing long chain HCs.

## CONCLUSION

The HC-SCR of lean NO<sub>x</sub> at low temperatures below 200 °C was remarkably improved using the Pt-catalyst supported on mesoporous silica (Pt/MPS). Such remarkable low-temperature activity of Pt/MPS is primarily due to the acidity of MPS rather than the sizes of Pt-particles and mesopores. The kinetic investigation of HC-SCR of NO<sub>x</sub> over Pt/MPS elucidated that the NO<sub>x</sub>-conversion below 200 °C is determined by the oxidation of NO to NO<sub>2</sub> which is the rate-determining step. The acid-treatment of the supports generates new functional groups assignable to active protons incorporated with the supports and makes the Pt-catalysts increase the activities. The active protons on the supports which may be acting as the Brønsted-acid sites probably influence the rate-determining step. It was also found that the HC-SCR of lean NO<sub>x</sub> is perfectly achieved with stoichiometric C<sub>6</sub>-C<sub>16</sub> HCs over a wide temperature range from 170 °C to 400 °C. The present HC-SCR must be very useful for de-NO<sub>x</sub> of diesel-exhaust by means of pulse-injection of diesel-fuel into the exhaust.

## REFERENCES

- [1] Narula, C. K.; Daw, C. S.; Hoard, J. W.; Hammer, T. Materials issues related to catalysts for treatment of diesel exhaust. *Int. J. Appl. Ceram. Technol.*, **2005**, *2*, 452-466.
- [2] Iwamoto, M.; Yahiro, H. Novel catalytic decomposition and reduction of NO. *Catal. Today*, **1994**, *22*, 5-18.
- [3] Bell, V. A.; Feeley, J. S.; Deeba, M.; Farrauto, R. J. In situ high temperature FTIR studies of NO<sub>x</sub> reduction with propylene over Cu/ZSM-5 catalyst. *Catal. Lett.*, **1994**, *29*, 15-26.
- [4] Burch, R.; Millington, P. J. Selective reduction of nitrogen oxides by hydrocarbons under lean-burn conditions using supported platinum group metal catalysts. *Catal. Today*, **1995**, *26*, 185-206.
- [5] Iwamoto, M.; Fernandez, A. M.; Zengyo, T. Oxidation of NO to NO<sub>2</sub> on Pt-MFI zeolite and subsequent reduction of NO<sub>x</sub> by C<sub>2</sub>H<sub>4</sub> on In-MFI zeolite: a novel de-NO<sub>x</sub> strategy in excess oxygen. *Chem. Commun.*, **1997**, 37-38.
- [6] Shichi, A.; Satsuma, A.; Iwase, M.; Shimizu, K.; Komai, S.; Hattori, T. Catalyst effectiveness factor of cobalt-exchanged mordenites for the selective catalytic reduction of NO with hydrocarbons. *Appl. Catal. B-Environ.*, **1998**, *17*, 107-113.
- [7] Burch, R.; Watling, T. C. The effect of sulphur on the reduction of NO by C<sub>3</sub>H<sub>6</sub> and C<sub>3</sub>H<sub>8</sub> over Pt/Al<sub>2</sub>O<sub>3</sub> under lean-burn conditions. *Appl. Catal. B-Environ.*, **1998**, *17*, 131-139.
- [8] Schießer, W.; Vinek, H.; Jentys, A. Catalytic reduction of NO<sub>2</sub> over transition-metal containing MCM-41. *Catal. Lett.*, **1998**, *56*, 189-194.
- [9] Iwamoto, M.; Zengyo, T.; Hernandez, A. M.; Araki, H. Intermediate addition of reductant between an oxidation and a reduction catalyst for highly selective reduction of NO in excess oxygen. *Appl. Catal. B-Environ.*, **1998**, *17*, 259-266.
- [10] Nakatsuji, T.; Yasukawa, R.; Tabata, K.; Ueda, K.; Niwa, M. Catalytic reduction system of NO<sub>x</sub> in exhaust gases from diesel engines with secondary fuel injection. *Appl. Catal. B-Environ.*, **1998**, *17*, 333-345.
- [11] Centi, G.; Perathoner, S. Novel catalyst design for multiphase reactions. *Catal. Today*, **2003**, *79-80*, 3-13.
- [12] Irfan, M. F.; Goo, J. H.; Kim, S. D. Co<sub>3</sub>O<sub>4</sub> based catalysts for NO oxidation and NO<sub>x</sub> reduction in fast SCR process. *Appl. Catal. B-Environ.*, **2008**, *78*, 267-274.
- [13] Komatsu, T.; Tomokuni, K.; Yamada, I. Outstanding low temperature HC-SCR of NO<sub>x</sub> over platinum-group catalysts supported on mesoporous materials expecting diesel-auto emission regulation. *Catal. Today*, **2006**, *116*, 244-249.
- [14] Ioan, B.; Miyazaki, A.; Aika, K. On the kinetic and structure sensitivity of lean reduction of NO with C<sub>3</sub>H<sub>6</sub> over nanodispersed Pt catalysts. *Appl. Catal. B-Environ.*, **2005**, *59*, 71-80.
- [15] Bueno-Lopez, A.; Illan-Gomez, M. J.; Salinas-Martinez de Lecea, C. Effect of NO<sub>x</sub> and C<sub>3</sub>H<sub>6</sub> partial pressures on the activity of Pt-beta-coated cordierite monoliths for deNO<sub>x</sub> C<sub>3</sub>H<sub>6</sub>-SCR. *Appl. Catal. A-General*, **2006**, *302*, 244-249.
- [16] Botas, J. A.; Miguel, A.; Gutierrez-Ortiz, M. P.; Gonzalez-Marcos, J. A.; Gonzalez-Marcos, J. R.; Gonzalez-Velasco, Kinetic considerations of three-way catalysis in automobile exhaust converters. *Appl. Catal. B-Environ.*, **2001**, *32*, 243-256.
- [17] Marnellos, G. E.; Efthimiadis, E. A.; Vasalos, I. A. Mechanistic and kinetic analysis of the NO<sub>x</sub> selective catalytic reduction by hydrocarbons in excess O<sub>2</sub> over In/Al<sub>2</sub>O<sub>3</sub> in the presence of SO<sub>2</sub> and H<sub>2</sub>O. *Appl. Catal. B-Environ.*, **2004**, *48*, 1-15.

Received: August 30, 2009

Revised: October 26, 2009

Accepted: October 27, 2009

© Komatsu *et al.*; Licensee Bentham Open.

This is an open access article licensed under the terms of the Creative Commons Attribution Non-Commercial License (<http://creativecommons.org/licenses/by-nc/3.0/>) which permits unrestricted, non-commercial use, distribution and reproduction in any medium, provided the work is properly cited.